Available online at www.CivileJournal.org

Civil Engineering Journal

(E-ISSN: 2476-3055; ISSN: 2676-6957)

Vol. 7, No. 06, June, 2021

Experimental and Numerical Investigations on Flexural Behaviour of Prestressed Textile Reinforced Concrete Slabs

Dang Quang Ngo [1], Huy Cuong Nguyen [1*]

[1] *University of Transport and Communications, No.3 Cau Giay Street, Hanoi, Vietnam.*

Received 02 February 2021; Revised 26 April 2021; Accepted 08 May 2021; Published 01 June 2021

Abstract

Nowadays, concrete is mostly prestressed with steel. But the application of prestressing steel is restricted in a highly corrosive environment area due to corrosion of prestressing steel, leading to a reduction in strength and may cause sudden failure. Carbon textile is considered an alternate material due to its corrosive resistance property, high tensile strength, and perfectly elastic. Prestressing is also the only realistic way to utilize fully ultra-high tensile strength in carbon textile material. In this study, experimental and numerical analyses were carried out for the flexural behaviour of prestressed and non-prestressed carbon textile reinforced concrete slabs. This study also focuses on the influences of textile reinforcement ratios, prestressing grades on the flexural behaviour of carbon textile reinforced concrete (TRC). Fifteen precast TRC slabs were tested, of which six were prestressed to various levels with carbon textile. The obtained results show that prestressing textile reinforcement results in a higher load-bearing capacity, stiffness, and crack resistance for TRC slabs. The first-crack load of the prestressed specimens increased by about 85% compared with those of non-prestressed slabs. Three-dimensional finite element models were developed to provide a reliable estimation of global and local response. The modeling techniques accurately reproduced the experimental behaviour.

Keywords: Textile Reinforced Concrete; Prestressed Slabs; Carbon; Flexure.

1. Introduction

Textile reinforced concrete (TRC) is a new innovative material that uses mesh-like reinforcements combined with fine-grained concrete. Due to its non-corrosive textile reinforcement, made of alkali-resistant glass or carbon fibers, a minimum concrete cover is necessary to transfer bond stresses from the reinforcement to the concrete. High strength, ductility, and non-corrosiveness textile reinforcements make TRC very suitable for constructing thin-walled, lightweight shell structures [1]. The weight of textile concrete elements could be reduced by up to 45%, resulting in a reduced need for maternal resources. This material can also strengthen existing concrete structures as a repair layer and a protective function to prevent corrosion problems in RC structures [2]. Today, tensile strength up to 3000 MPa can be achieved depending on the fiber material. However, textile reinforcements' high strength property could not be effectively utilized due to concrete performances [3]. Concrete performs well under compression but will be easily cracked when subjected to tension, and reinforcement becomes mostly effective only after cracking occurs. In this case, the low reinforcement ratio and high strength of textile reinforcement, together with a lower modulus of elasticity, are disadvantageous for applying TRC structures. The first crack that forms becomes relatively wide, and subsequent cracks appear, resulting in a less stiff structure, and these may violate serviceability limit state requirements

* Corresponding author: nguyenhuycuong@utc.edu.vn

http://dx.doi.org/10.28991/cej-2021-03091712

In order to avoid or limit the cracks in concrete and, at the same time, utilize the actual tensile strength of the textile and make it act more actively, the TRC members should be prestressed. In the case of textile reinforcements, pre-tension prestressing may be the most appropriate method. This new approach is expected to increase the cracking load of TRC structures; thus, the uncracked state's serviceability is improved. On the other hand, the textile reinforcements are behaving linearly elastic until rupture. This property is particularly suitable for prestressing techniques. Prestressed TRC leads to more slender and thereby more economical and durable structural elements. Since TRC is still a relatively new construction material, which has not yet been standardized, little research was reported in this area, especially for the prestressed TRC structures. Krüger [4] conducted a study to investigate the bond behaviour of textiles used for prestressing in fine-grained concrete under different conditions. Following epoxy impregnation, the prestressing of the roving leads to enhanced bond strength and stiffness. Krüger also reported that using alkali-resistant glass textiles as a prestressing element is not practical due to creep and a low static fatigue limit. Zdanowicz [5] compared bond behaviour between prestressed specimens and non-prestressed control specimens and concluded that chemical prestressing positively influences the bond behaviour of concrete with textile reinforcement. In these tests, the chemically prestressed specimens reached 24% higher bond strength than non-prestressed ones.

Peled [6] found that pre-tensioning of fabrics and the time at which the tension is removed can significantly influence the composite's performance depending on yarn properties, mainly the viscous–elastic properties and fabric geometry. Yunxing [7] experimentally investigated the influences of textile layers, prestress levels, and short steel fibers on the tensile behaviour of carbon TRC. It was found that evident increases in first-crack stress and tensile strength were observed with increasing prestress grades. Therefore, the capacity of TRC composites at the serviceability limit states can be upgraded by exerting a prestressing force on the textiles. Gopinath [8] carried out a study to determine the uniaxial tensile behaviour of prestressing TRC plate with two types of alkali-resistant glass textiles, woven and bonded, and their combinations. From this study, TRC with mechanically stretched textile exhibited lower crack width and average crack spacing than with manually stretched textile.

Yunxing et al. (2018) [9, 10] conducted experimental studies on the influences of the number of textile layers, prestress grades of textile on the flexural behaviour of basalt and carbon textile-reinforced concrete plate. The presence of prestressing or steel fibres improved first-crack and ultimate stresses of the TRC specimens. Compared with the first-crack stress, a more pronounced enhancement in the ultimate stress was achieved by adding steel fibres. Reinhardt et al. (2003) and Reinhardt & Krüger (2004) [11, 12] dealt with carbon and glass TRC slabs' flexural behaviour and reported that the impregnated carbon is very suitable for prestressing. The most considerable effect of prestressing is that the initial strain of fabric is anticipated and that deflection and crack width after first cracking is minimized. Meyer [13] studied the flexural behaviour of the prestressed aramid TRC, in which the textiles were evenly placed along with the thickness of the specimens. In their work, the prestress delayed the generation of cracks and improved the post-cracking flexural stiffness and bearing capacity of the specimens but decreased the ductility. Liu [14] investigated the flexural properties of basalt TRC slab with pre-tension, short carbon, steel, and AR-glass fibers through three-point bending in a utilizing drop-weight impact setup. In this research, the flexural impact responses of the basalt TRC with flexural strength, flexural modulus, maximum strain, and toughness were improved by pre-tension. Yunxing [15] also investigated the flexural behaviour of preloaded reinforced concrete beams strengthened with a prestressed carbon TRC plate under various preloading conditions. The test results showed that the prestressed carbon TRC plates could significantly increase the cracking and ultimate loads and effectively inhibit the propagation of cracks.

Despite those advantages, the number of practical applications using prestressed TRC is still negligible in the current state. One explanation for this situation is the available design codes and guides do not provide any recommendations for TRC since fundamental studies, and relevant applications are still limited. Although there are reference guidelines for determining the mechanical behaviour of TRC [16-19], there is no standard. Therefore, investigations are needed to characterize and understand the structural behaviour of the TRC prestressed slab. The overall objective of this research is to investigate the flexural performances of non-prestressed and prestressed TRC slabs. The influences of the number of textile layers, prestress grades on the flexural behaviour of carbon TRC slabs are also discussed in this paper. Based on the four-point bending tests, the load–deflection relationship, cracking mechanisms, and failure modes of each experimental case are presented and analyzed. Furthermore, experimental results are required to validate analytical models' ability to capture the critical response characteristics of the non-prestressed and prestressed TRC slabs.

The brief research methodology flow chart, as shown in Figure 1, has been adopted to achieve the study's objective. The following section will present the full description of the two phases of the experimental program. Phase 1 presents the detailed preparation of the material properties, including fine-grained concrete, carbon textile reinforcement, and bond strength between textile and fine-grained concrete. The 2nd phase is the laboratory experiment: casting two sets of specimens, test set-up, and analyzing the experimental results. The finite element modeling was continuously conducted to validate the experimental results.

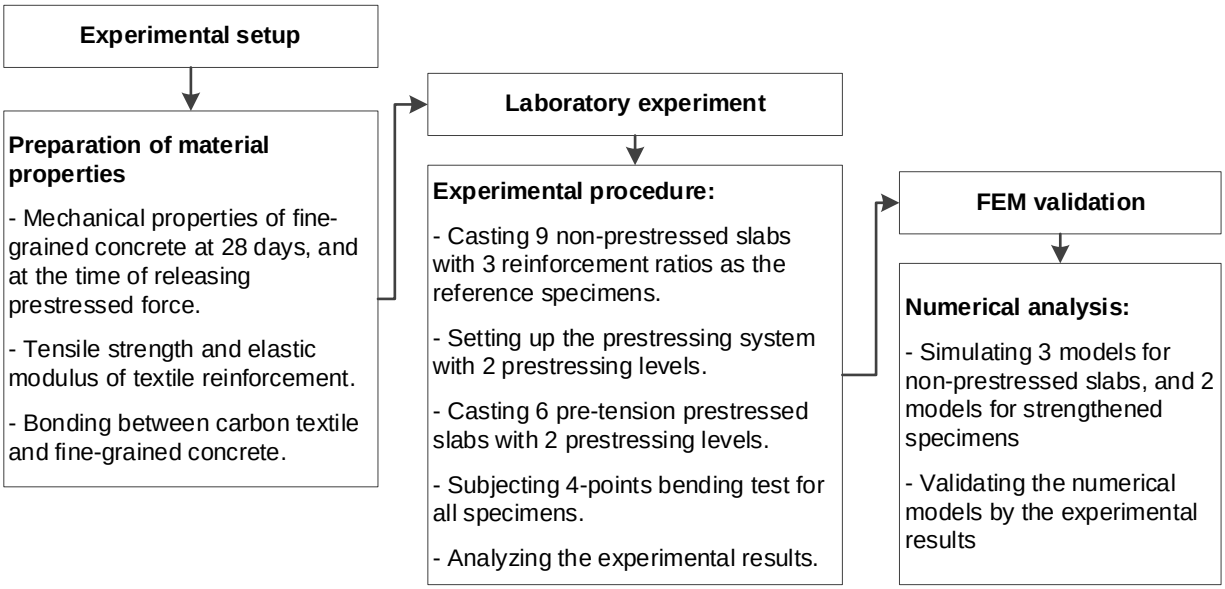

Figure 1. Research methodology flow chart

2. Experimental Investigation

2.1. Specimens and Test Description

In this study, all the carbon TRC specimens had the same dimension of 900 mm (length) × 150 mm (width) × 40 mm (depth). Two sets of TRC specimens were tested, corresponding to the non-prestressed and prestressed slabs. In the first set, the TRC slabs use 1, 2, and 3 carbon textile layers, corresponding to the longitudinal reinforcement ratio of 0.34, 0.69, and 1.05%, respectively. In the 2nd set, six specimens were applied by prestressing force, corresponding to 50 and 70% tensile force of the textile layer in the uniaxial test. The initial prestressing values were selected based on the recommendations of conventional prestressed reinforced concrete theory. For each experimental case, three nominally identical specimens were manufactured. Specimens were named following the notation P*x*L*y*Nz, where *x* = prestressed level in percentage, *y* = number of textile layers, and *z* = specimen number. For example, the label P50L1N2 represents the 2nd specimen with one layer of carbon textile applied by the prestressing level of 50%. The detailed information for each specimen is mentioned in Table 2.

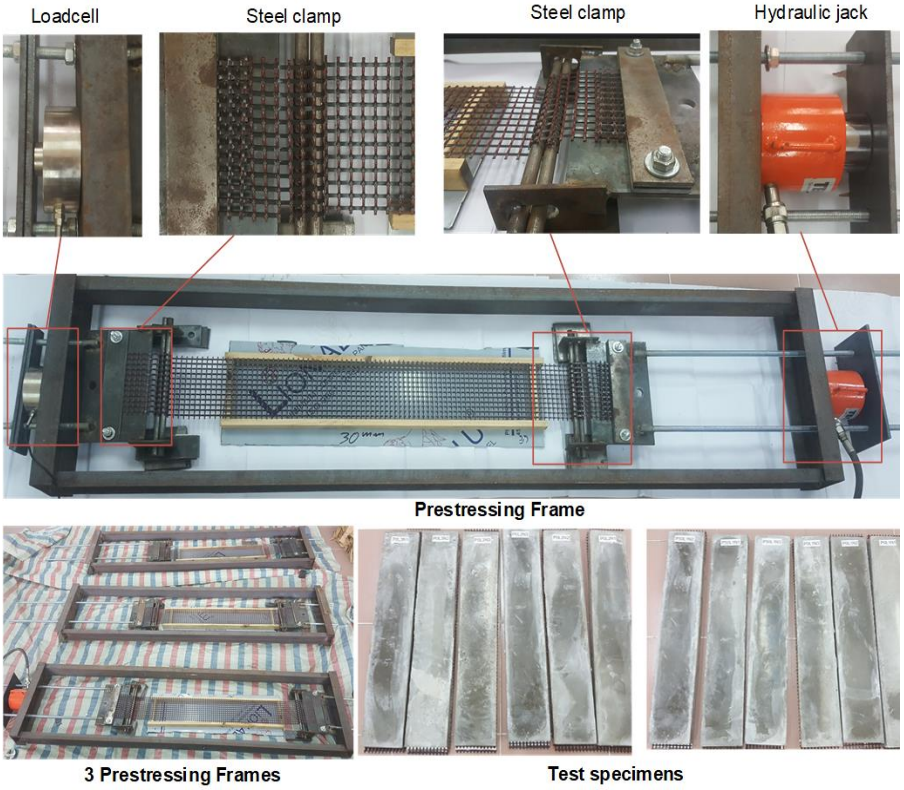

Figure 2. Prestressing frames and test specimens

Figure 2 shows the prestressing frame as prepared for a uniaxial prestressing of textile. The clamps and the hydraulic jack can be seen in the frame with a total size of about 2.0 × 0.5 m. The preparation process was initiated by fixing all the textiles on the prestressing frame at both ends of the device, and textiles were wrapped around two smooth rollers, which were then placed in the steel clamp. The pre-tension force was applied to the textile reinforcement by the hydraulic jack and was measured by the load cell fixed at the other end of the frame. Based on the material properties of carbon textile, the elongation of textile reinforcement was also measured to control the pre-tension force. After reaching the textiles' prescribed prestress value, the chute at the tension end was fixed by the adjusting nut. Subsequently, fine-grained concrete was mixed and directly poured into the mold. Then, the mixture was vibrated thoroughly, and the top surface was smoothed by using a metal spatula. The TRC slabs were covered with wet cloths after the matrix was initially set. The prestressed ones were allowed to harden for 14 days before releasing the pre-tension force. All the slabs were then removed from their molds and cured until testing was performed after 28 days.

2.2. Material Properties

The fine-grained binder systems with a maximum grain size of 0.63 mm were designed explicitly for carbon textile application. The high-performance plasticizer and fly ash were added to achieve an excellent flowing capability of the concrete to ensure proper penetration of the fabrics' small gaps. The fine-grained concrete was mechanically characterized by testing six 40×40×160 mm prisms. The average flexural strength and average compressive strength at 28 days were equal to 6.95 and 47.5 MPa, respectively. The average flexural strength and compressive strength at 14 days (at the time of releasing prestressed force) were identical to 5.72 and 38.7 MPa, respectively.

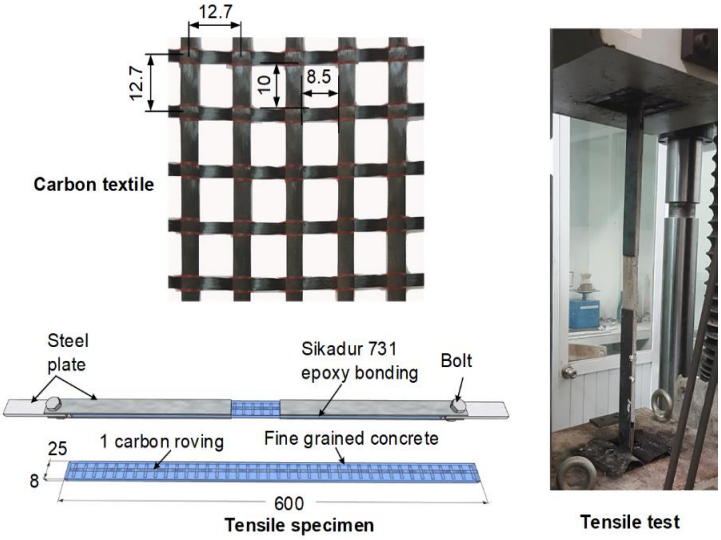

Figure 3. Carbon textile and TRC specimen for the uniaxial tensile test

In this study, the carbon textile reinforcement SITgrid017 was used. The carbon fiber yarns, having a count of 3200 tex, were processed in the warp and weft directions with a distance of approximately 12.7 mm between them. Each carbon roving consists of 48.000 fibers and has a cross-sectional area of 1.808 mm² (in both directions). A textile weighting unit area of roughly 578 g/m^2 was produced. The geometrical and mechanical characteristics are collected in Table 1. According to the Recommendation of RILEM TC 232-TDT [18], the tensile strength and elastic modulus of the fiber were measured through tensile tests on the uniaxial tensile specimens (Figure 3) and were equal to 2890 MPa, and 185 GPa, respectively.

Table 1. The geometrical and mechanical characteristics of SITgrid017 textile

Geometric				Mechanical characteristics	
Roving distance (mm)	**Rovings/m**	**Mesh size (mm)**	**Roving area (mm^2)**	**Tensile strength (MPa)**	**Elastic modulus (GPa)**
12.7 ×12.7	78	10 × 8.5	1.808	2890	185

2.3. Test Setup and Instrumentation

All the tests were conducted in the Structural Engineering Laboratory at the University of Transport and Communications, Vietnam. Specimens were monotonically loaded with four-points bending, using displacement controlled method, with a loading rate of 1 mm/min. The clear span of all the slabs was kept constant at 450 mm, and the shear span was 150 mm. The schematic view and a view of the test setup are shown in Figure 4. A linear variable

differential transformer (LVDT) was installed on the slab's bottom surface to measure its deflections during the test. Moreover, strain-gauges were used to record compressive and tensile strains of concrete at upper and lower surfaces during the experiment. A computer-based data acquisition system was used to record the load from the load-cell, the deflection from LVDT, and strain-gages.

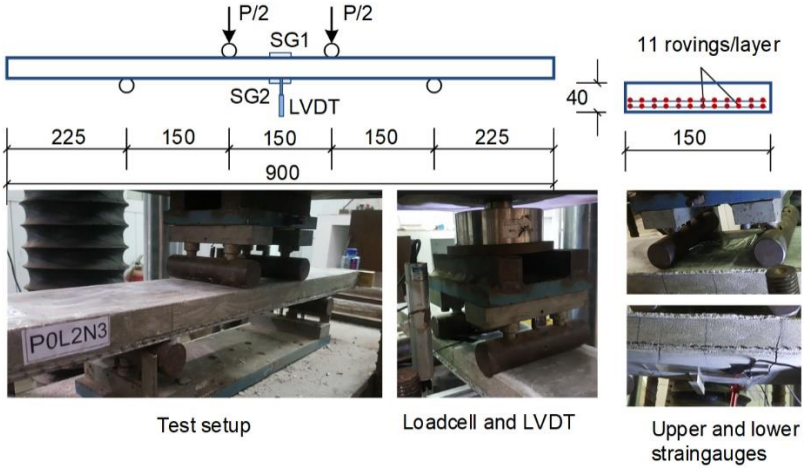

Figure 4. Test setup

2.4. Test Results

The load versus deflection curves for Set 1 and Set 2 are presented in Figures 5 and 7, respectively. Table 2 shows a summary of the load-deflection in cracking and ultimate of all test specimens. Besides, failure modes and crack patterns of tested slabs are illustrated in Figure 6 and Figure 8. The experimental results showed that the non-prestressed and prestressed slabs with one textile layer failed due to the carbon textile rupture (Figures 6-a and 8). Besides, the non- prestressed slabs with 2 and 3 textile layers failed due to the crushing of the concrete in the compression zone before rupture of the textile reinforcement (Figure 6-b).

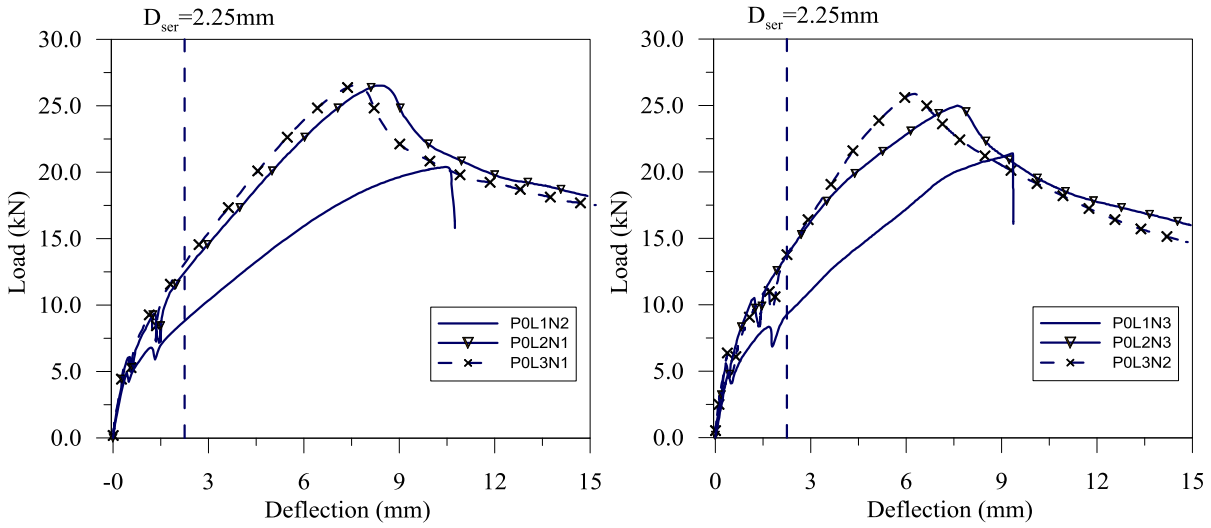

Figure 5. Load-displacement of Non-Prestressed Slabs

Figure 5 compares the load-deflection of non-prestressed slabs with 1, 2, and 3 fabric layers. All slabs show similar load-bearing behaviour in the first stages. The load-deflection curves indicate a linear elastic behaviour, up to the point of first flexural crack appears, at a load level of 4 to 6 kN. The average cracking loads in 2 and 3-layers slabs are 14 and 18% higher than those of 1 layer slabs. The slabs' stiffness decreased after the first cracks, resulting in more significant deflection, especially in 1-layer slabs. Due to the bond between textile roving and fine-grained concrete, tensile stress was developed in the concrete until the fine-grained concrete's tensile strength is reached once more. With an increase of the tension force, an additional crack occurred in all types of tested slabs. After the cracks' appearance, the load-deflection curves showed small drops due to the transfer of tensile force from fine-grained concrete to textile reinforcement. The tensile stress in textile reinforcement will increase sharply, resulting in a significant increase in tensile strain. However, the slabs were loaded under displacement-control manner, the tensile strain in textile reinforcements could not reach the required level immediately. Hence, the applied load will decrease suddenly for a short while until the tensile stress increase again.

In 1-layer slabs, by a load increase, the rovings are strained up to their tensile strength. In this stage, the crack pattern was stabilized, no further cracks occur, but the most significant crack expanded larger. Then, the textile reinforcement was continuously broken, resulting in the flexural failure mode with rupture of textile reinforcement. It can be seen from Figure 5 that after cracking, the specimens with more textile layers had higher stiffness and hence had higher bearing capacity at the same mid-span deflection, which can also be proved by the results listed in Table 2. In contrast to 1-layer slabs, the non-prestressed slabs with 2 and 3 fabric layers exhibited the concrete's crushing in the compression zone at the defection of around 7 mm. After the two and three-layers specimens reach their ultimate capacity (approximately 25.5 kN), their curves show a slight but constant decrease. This is due to the fact that the concrete could not carry the significant compression force, and the concrete zone fails more and more. This also means that the textiles' full tensile capacity cannot be used because of the weakness of the compression zone.

Table 2. Load, deflection, and modes of failure comparison for all specimens

Set	Slab	Cracking			Ultimate			Failure mode	Energy dissipation (kN.mm)
		D_{cr} (mm)	P_{cr} (kN)	$P_{cr,avg}$ (kN)	D_u (mm)	P_u (kN)	$P_{u,avg}$ (kN)		
Set 1: Non pre-stress	P0L1N1	0.43	5.50	5.28	9.36	21.40	20.51	Textile rupture	16.29
	P0L1N2	0.43	5.48		10.44	20.40			15.76
	P0L1N3	0.32	4.97		10.34	19.75			16.43
	P0L2N1	0.53	6.10	6.02	8.25	26.41	25.36	Concrete crushing	20.91
	P0L2N2	0.49	6.37		8.17	25.38			19.35
	P0L2N3	0.33	5.60		7.61	24.29			24.42
	P0L3N1	0.48	6.10	6.23	7.50	26.51	25.79	Concrete crushing	24.05
	P0L3N2	0.38	6.37		6.28	25.88			28.13
	P0L3N3	0.35	6.22		7.25	24.99			23.96
Set 2: Pre-stress	P50L1N1	0.65	9.89	9.68	6.32	22.40	21.92	Textile rupture	30.70
	P50L1N2	0.52	9.15		6.78	22.11			31.57
	P50L1N3	0.63	10.11		5.29	21.24			30.83
	P70L1N1	0.67	10.14	9.86	5.72	20.75	21.33	Textile rupture	31.25
	P70L1N2	0.62	10.01		4.92	21.69			34.04
	P70L1N3	0.53	9.44		6.05	21.55			30.44

Abbreviations:

D_{cr}: displacement at cracking. D_u: displacement at failure.

P_{cr}: corresponding load at cracking. P_u: ultimate load at failure.

$P_{cr,avg}$: averaged load at cracking. $P_{u,avg}$: averaged ultimate load at failure.

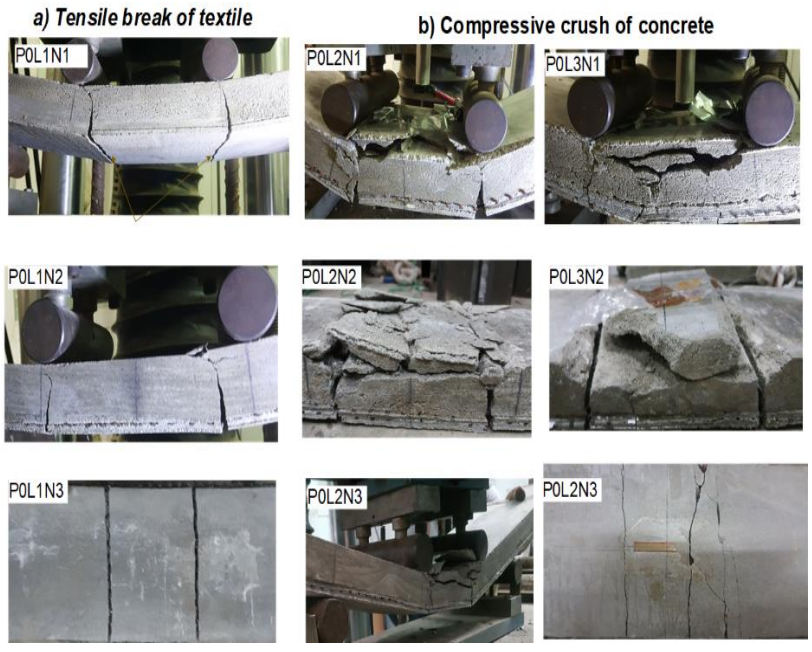

Figure 6. Crack patterns of test specimens in Set 1

Figure 7 represents the influences of prestressing grades on the bending behaviour of TRC slabs. The behaviour of all prestressed specimens in Set 2 also presented a typical flexural failure mode, consisted of three stages, namely: (a) the un-cracked stage, (b) the cracked stage, and (c) the failure stage. The load was linear up to the first flexural crack initiation in pure bending span, followed by a non-linear behaviour up to failure. The average first-crack load of the prestressed specimens increased by 83.3 and 86.7%, respectively, compared with those of non-prestressed slabs. The compressive pre-strain in the fine-grained concrete induced by the prestressing force increased the first-crack stress and enhanced the flexural modulus. Since the carbon textile has no plastic capacity, the TRC specimens failed when the reinforcements reach their tensile strength. All textile rovings were continuously broken in a brittle manner. Before breaking, there was no sign of compressive failure in the top edge of TRC slabs. It should be noted that the effectiveness of prestressing force grades (i.e., 50 and 70%) in cracks resistance is not much different.

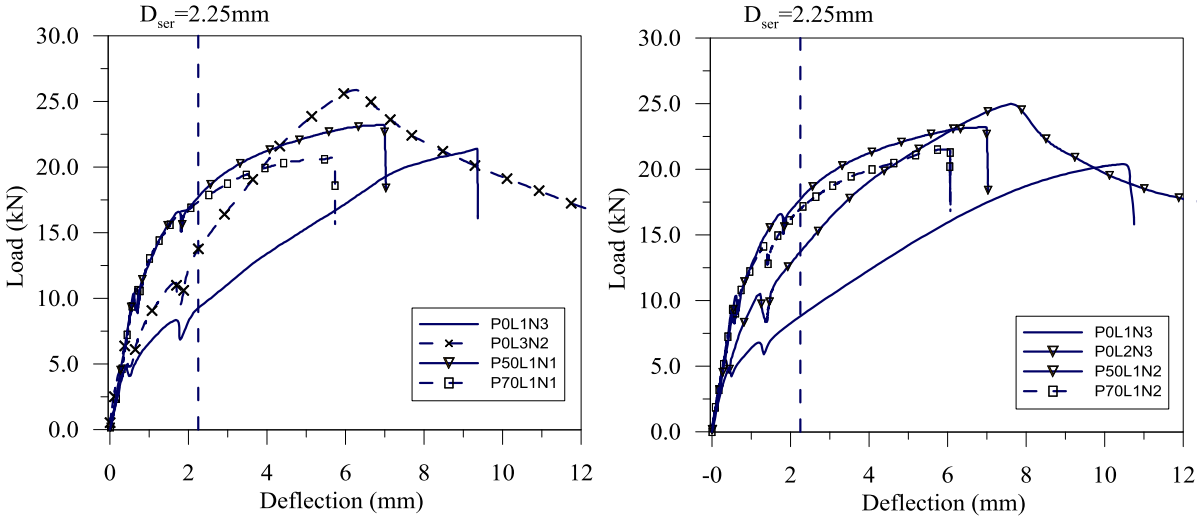

Figure 7. Comparison in load-displacement of Non-Prestressed and Prestressed Slabs

As shown in Table 2, prestressing forces on the textile also slightly improved the bearing capacity of the TRC specimens and reduced the ultimate deflection. This can be explained by the complexity of the tensile strength of textile rovings. The concrete cracks along the reinforcement lead to damage in the rovings and cause a decreasing strength of the component. The main effects responsible for this loss of strength are the lateral pressure and the bending stresses of the filaments at the crack edges [1]. As displayed in Figure 8, the crack's width in prestressed specimens before failure was much smaller than that in non-prestressed slabs. The smaller cracks resulted in the larger tensile strength of textile rovings. The comparison of data above indicated that the prestress on textile improved the first-crack and ultimate load capacities of the TRC specimens.

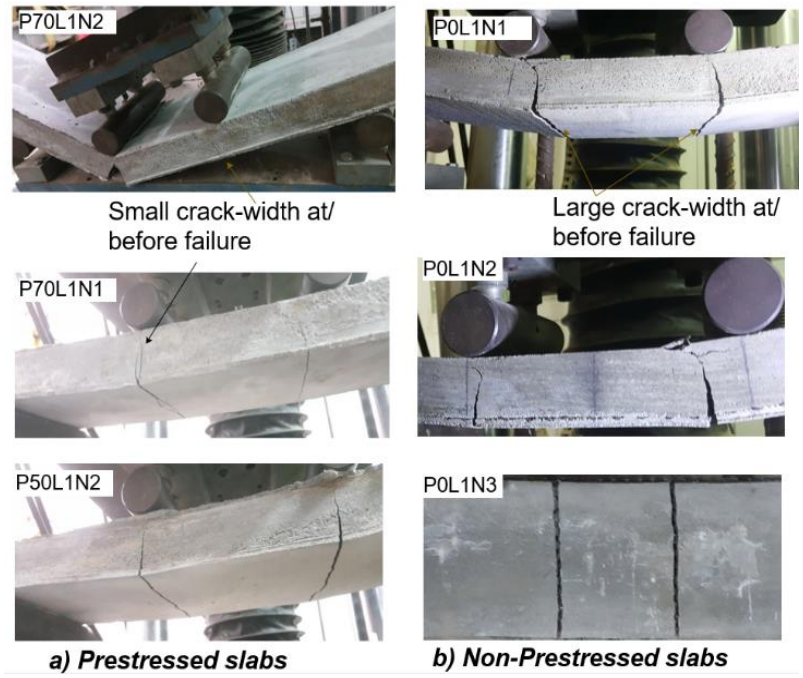

Figure 8. Comparison of Crack patterns of slabs with 1 textile layer in Set 1 and Set 2

In order to apply TRC slabs in construction, the deflection of these structures is one of the checks that should be performed for serviceability limit state design. In this test, the clear span of all the slabs was kept constant at 450 mm. This research also compares the load capacity and the energy dissipation of prestressed and non-prestressed slabs at a deflection level of 2.25 mm, corresponding to 1/200 tested span. As shown in Figure 7 and Table 2, the average load in prestressed slabs is 85.6 and 91.2 % higher than those of non-prestressed slabs. Energy dissipation is estimated by the area under the load - defection curves. The average energy in prestressed slabs is 92 and 97 % higher than those of non-prestressed slabs with 1 fabric layer. The energy in 50% prestressed slabs is also 44% and 48% higher than those of non-prestressed slabs with 2 and 3 fabric layers.

3. Numerical Investigation

3.1. Finite Modeling

The numerical analysis using ABAQUS 6.12-1 software was carried out to predict the ultimate capacity, the mechanical behaviour of the structures and compared to the measured results. A total of five FE models was performed for both prestressed and non- prestressed specimens. A full view of specimen P0L1-FEM is shown in Figure 9 for reference. Due to the symmetry of the specimen geometry and loading, only a quarter of the specimens were modelled to save the calculation time. The slab was restrained at the support employing hinges. The loading was applied continuously in the form of the displacement control manner.

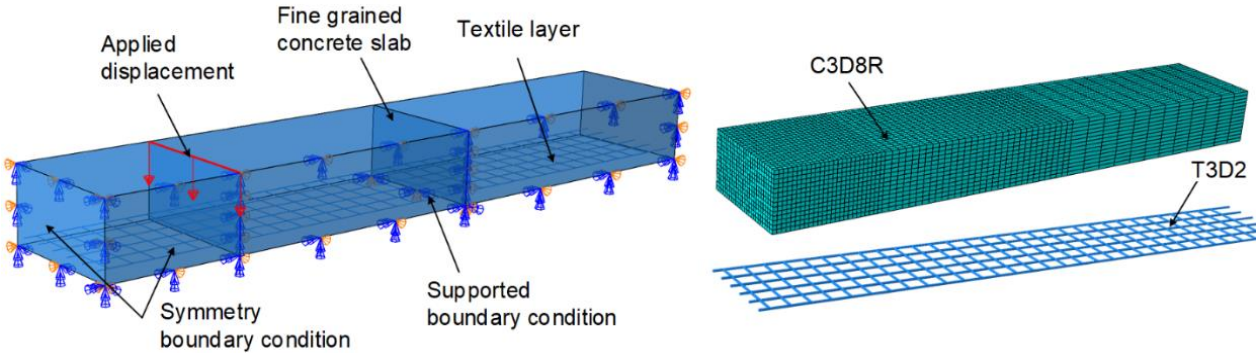

Figure 9. FE model of P0L1-FEM TRC slab

Two components of the specimen (fine-grained concrete slab and textile reinforcement) were modelled separately and assembled to make a complete specimen model. Furthermore, element types, mesh sizes, boundary conditions, and load applications have been chosen so that the simulation results could agree with ones from experiments. The material nonlinearity is included in the FE analysis. The element type used for the numerical discretization in the 3D concrete parts is the C3D8R element from the ABAQUS library [20]. The T3D2 (3-noded quadratic 2-D) truss elements are used to generate textile reinforcements. Figure 9 also shows the meshing of the FE model for the concrete slab carbon textile. To achieve reliable results, the fine mesh was used in the pure bending zone. In these models, embedded textile reinforcement is assumed to be perfectly bonded to the concrete element, which implies infinite bond strength at the interface between the concrete and the reinforcement.

The material behaviour of single textile roving can be appropriately described with a brittle elastic isotropic material. The fiber strength controls the tensile failure of textile in the fiber direction. As seen from Figure 10-a, the textile material has captured elastic-brittle materials' response, and it showed no appreciable plastic deformation before failure. The stress is linear up to the tensile strength and does not exhibit yielding behaviour. After reaching the tensile strength, the stress drops sharply to zero, representing the textile's rupture. The input parameters were assigned according to the experimental data.

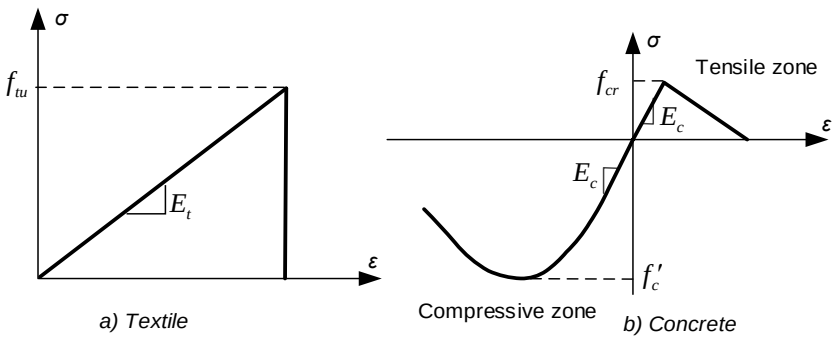

Figure 10. The stress-strain relationship for the textile and concrete materials

Table 3. The values of the parameters used in CDP model for concrete

E_c (MPa)	f_{cr} (MPa)	E_c (MPa)	υ	K_c	ϵ	$\frac{\sigma_{b0}}{\sigma_{c0}}$	ψ	μ
47.5	6.95	32600	0.2	2/3	0.1	1.16	31°	1E-5

The Concrete Damaged Plasticity (CDP) model was adopted to model the inelastic stress-strain relation in the compressive and tensile regions (Figure 10-b). This model consists of the combination of non-associated multi-hardening plasticity and scalar damaged elasticity to describe the irreversible damage that occurs during the fracturing process [20]. For compressive behaviour, the uniaxial stress-strain curve of Eurocode 2 [21] is selected to determine yield stress and inelastic strain. For the tensile behaviour of concrete, the tensile stress was assumed to increase linearly to the strain until the concrete crack. After the cracking of the concrete, tensile stress decreases linearly to zero. In the CDP model, five parameters control the evolution and the shape of the yield surface and the flow potential. These parameters' default values are taken as a recommendation of the CDP model in ABAQUS user's manual [20]. These material properties that have been assigned in the CDP model are summarized in Table 3.

In total, five three-dimensional finite element models were developed. Three of them, denoted as P0L1-FEM, P0L2-FEM, and P0L3-FEM, were non-prestressed slabs with 1, 2, and 3 textile layers, respectively. Two models, namely P50L1-FEM and P70L1-FEM, were prestressed slabs. In the prestressed models, the function "predefined field" in ABAQUS was used to introduce prestressing in the textile reinforcement. The prescribing field stress variable values were defined as 1400 MPa and 2000 MPa, corresponding to 50% and 70% prestressed stress in textile reinforcement (Figure 11).

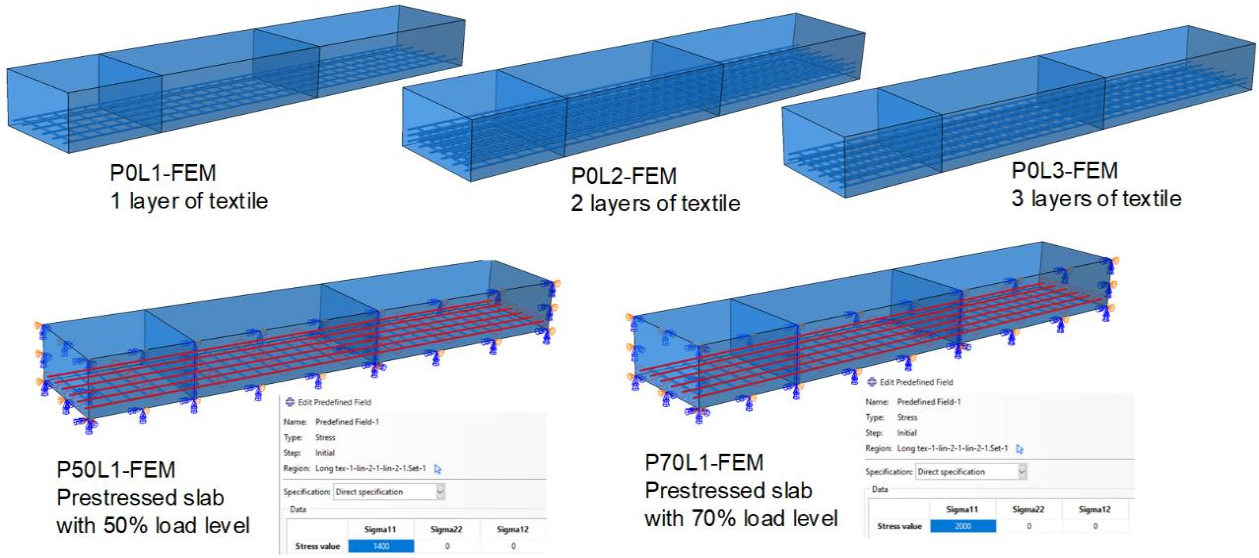

Figure 11. All 5 finite element models

3.2. Verification of the FE Models

The load-deflection curves of all five models are plotted in Figure 12-a. In the case of 3 non-prestressed slabs, it is apparent that increasing the number of layers tends to enhance the overall capacity of the TRC slabs. At the same level of applied load, a high amount of textile reinforcement corresponds with a lower deflection. Therefore, the performance of the TRC slabs in the service limit state is increased. To verify the FE models, the numerical and experimental load-deflection curves are also compared with each other and illustrated in Figure 12-b, c, d. It can be seen that the cracking and ultimate loads obtained from the FE model correlate relatively well to those from the tests. A comparison between the cracking and ultimate loads is presented in Table 4. The average discrepancy in cracking and ultimate load values between experimental and FE predictions were found to vary from 2 to 13%.

As clearly seen in Figure 12-b, the comparison between FE results and experimental data for one textile layer slab shows a good correlation for whole curves. The P0L1-FEM slab behaved like an elastic material up to the first cracking strength. Then, the first cracks in the concrete appear exposed by a sudden variation of the load. The stabilization of the cracking follows this process and subsequently increasing tensile stress in textile reinforcement. The stiffness of the slab is reduced, and the textile reinforcement stress increases until the breaking point. The breaking of carbon textile in the P0L1-FEM model is also numerically depicted by the Von Mises stress distribution shown in Figure 13-a. As can be seen, at the applied load of 19.89 kN, the tensile stresses of the carbon layer in the pure flexural zone exceeded the textile's tensile strength. Then, with the increase of the applied displacement, the tensile stress of

textile at these positions dropped suddenly to zero, representing textile reinforcement's rupture. It is also noted that the compressive stress in the concrete slab was much smaller than the compressive strength. It shows the good agreement in failure mode to the experiment results.

Table 4. Comparison of experimental and numerical results

Set	Slab	Cracking load				Ultimate load			
		Experiment		P_{FEM} (kN)	FEM/ EXP	Experiment		P_{FEM} (kN)	FEM/EXP
		P_{cr} (kN)	$P_{cr,avg}$ (kN)			P_u (kN)	$P_{u,avg}$ (kN)		
Set 1: Non-Prestress	P0L1N1	5.5	5.32	5.62	1.06	21.4	20.51	19.89	0.97
	P0L1N2	5.48				20.4			
	P0L1N3	4.97				19.75			
	P0L2N1	6.10	6.02	6.43	1.07	26.41	25.36	28.65	1.13
	P0L2N2	6.37				25.38			
	P0L2N3	5.60				24.29			
	P0L3N1	6.10	6.23	6.78	1.09	26.51	25.79	28.99	1.12
	P0L3N2	6.37				25.88			
	P0L3N3	6.22				24.99			
Set 2: Prestress	P50L1N1	9.89	9.72	14.35	1.48	22.4	21.91	22.28	1.02
	P50L1N2	9.15				22.11			
	P50L1N3	10.11				21.24			
	P70L1N1	10.14	9.86	17.35	1.76	20.75	21.33	24.04	1.13
	P70L1N2	10.01				21.69			
	P70L1N3	9.44				21.55			

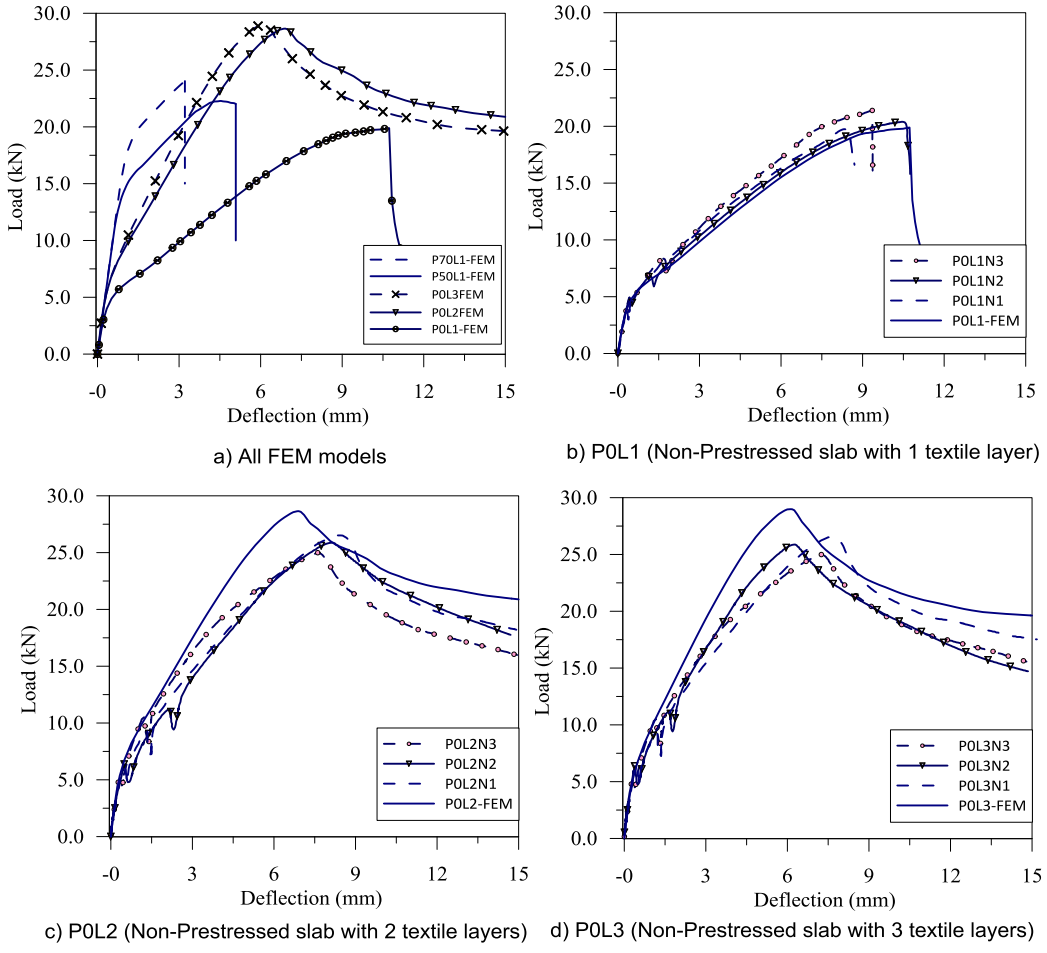

a) All FEM models

b) P0L1 (Non-Prestressed slab with 1 textile layer)

c) P0L2 (Non-Prestressed slab with 2 textile layers)

d) P0L3 (Non-Prestressed slab with 3 textile layers)

Figure 12. Comparison of numerical and experimental results of the Non-Prestressed slabs in Set 1

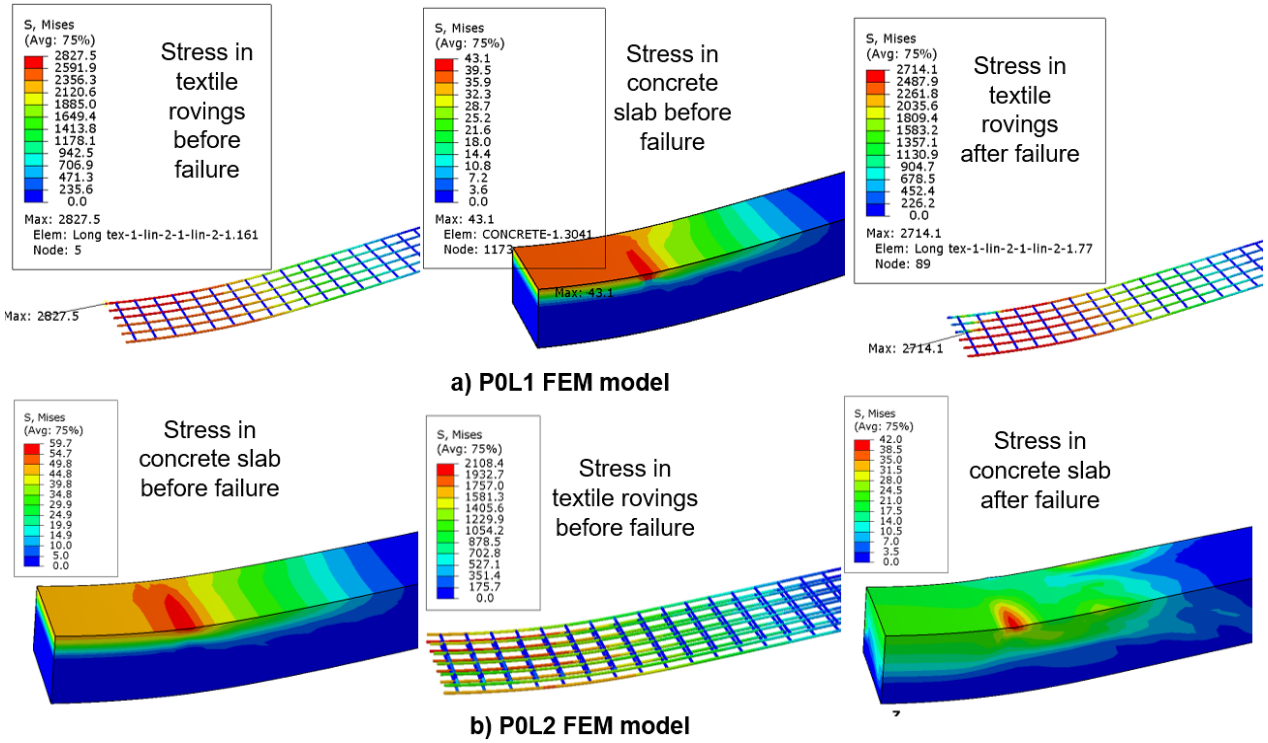

Figure 13. Von Mises stress distribution in concrete and textile in non-prestressed model

Moreover, the models of the slabs using 2 and 3 layers of textile reinforcement were analyzed. As expected, their behaviour was very similar to the case of 1 layer of textile. The elastic phase is almost identical in all cases, as shown in Figure 12. The models with 2 and 3 textile layers had the same failure mode, the crushing of concrete slabs before reaching the textile's rupture in tension. Figure 13-b shows that, at failure points of the P0L2-FEM model, the textile stress is only 2108 MPa. Simultaneously, the compressive stresses in extreme concrete fibers were even higher than the compressive strength of concrete due to the confinement in local positions (under the applied load points). After this point, the stress distribution in concrete changed dramatically, representing the crushing in concrete. This leads to a gradual decrease of the load-deflection curves. The main differences between FEM models were tested specimens were the models' stiffness after cracking and the ultimate load. As seen in Figure 12-c,d, both models, P0L2-FEM, and P0L3-FEM, were slightly stiffer than the actual slabs after cracking point.

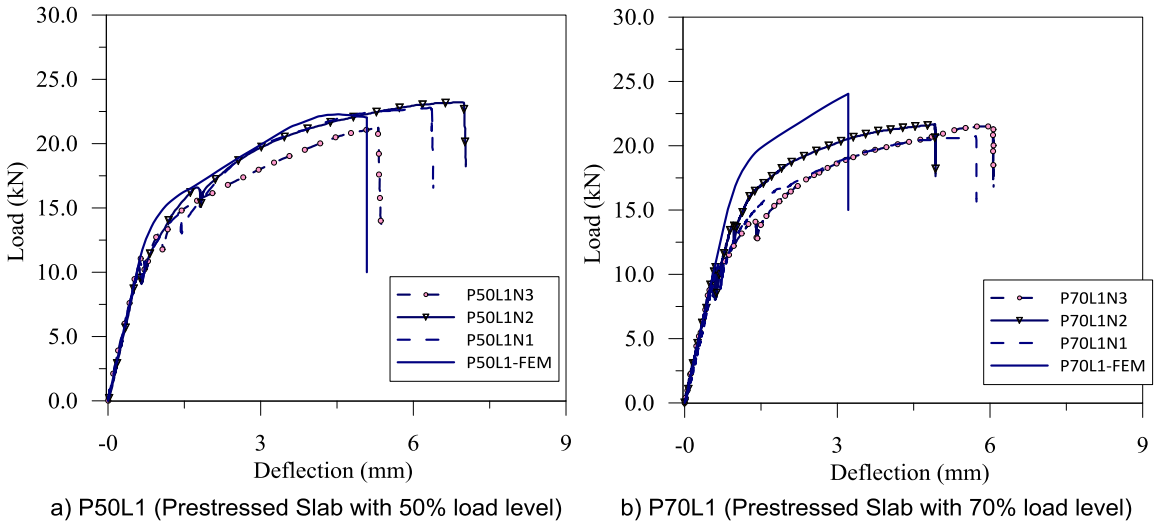

Figure 14. Comparison of numerical and experimental results of prestressed slabs in Set 2

Figure 14 contains a comparison between the load-deflection curves predicted by ABAQUS and the test results for prestressed slabs. The cracking load in P50L1-FEM and P70L1-FEM are respectively 48 and 76% higher than those of tested specimens. This could be explained by the reason that the prestressing force does not remain constant during the manufacturing process. The loss of stress in textile reinforcements was not well-controlled and also not implemented

in ABAQUS models. However, the ultimate load in these models are marginally bigger than those at tested slabs, corresponding to a difference of 2% in P50L1-FEM. The large difference in stiffness of FE model also caused the much smaller deflection at the failure point. In the P50L1-FEM model, the textile was ruptured at displacement of 3.4 mm, while those in the experiments were was approximately 6 mm.

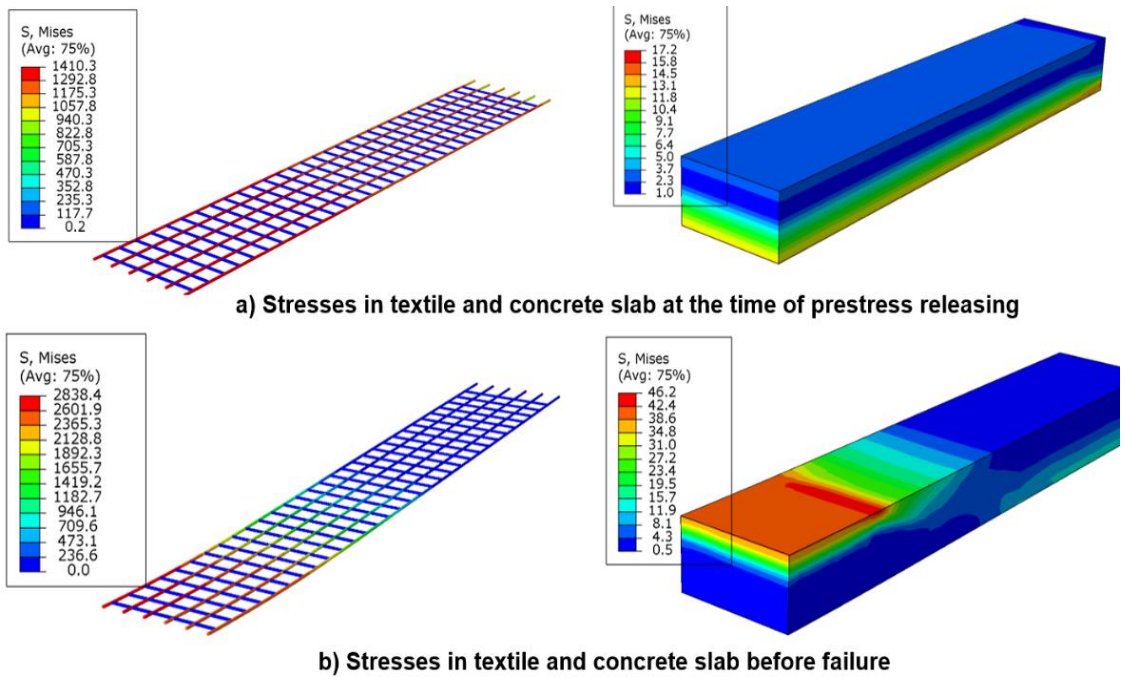

Figure 15. Von Mises stress distribution in concrete and textile in prestressed model P50-FEM

Figure 15 represents the Von Mises stress distribution in concrete and textile in prestressed model P50-FEM. When releasing the prestress load, the stress in the longitudinal rovings was uniformly distributed approximately 1400 MPa. The stress in concrete was also uniformly dispersed in the whole slab. This can be explained by the bond between the concrete and textile reinforcements are assumed to be perfect (no-slip) in the FE analyses. The stresses in the bottom fibers of the concrete slab were transferred from compression to tension by increasing the applied loads. As can be seen in Figure 15-b, both two prestressed models were failed due to textile rupture. At this point, the tensile stresses of the carbon layer in the pure flexural zone exceeded the textile's tensile strength, while the compressive stress in concrete was still smaller than the compressive strength.

4. Conclusions

This paper presents the experimental and numerical results obtained for the flexural behaviour of carbon TRC slabs. Both the analytical and experimental works demonstrate that it is possible to use carbon textile to replace steel bars to reinforce and prestress the precast slabs. The influences of the number of textile layers and prestressing grades on the flexural performances are investigated using four-point bending tests. Following conclusions could be drawn from the current investigation:

For the non-prestressed slabs, increasing the number of textile layers has a significant effect on overall behaviour. With the increase in the number of textile layers, an improvement in the specimens' bearing capacity and a smaller reduction in the flexural stiffness of the cracked specimens were observed. However, due to the limitation of the concrete compression capacity limits, the textiles' tensile strength was not fully utilized. The specimen's failure mode changed from textile rupture in 1 layer specimens to concrete crushing failure in 2 and 3 layers specimens.

Prestressing force on textile contributes to the evident improvement on first-crack load, but only slightly influences the ultimate tensile strength of TRC. The average first-crack load of the prestressed specimens increased by 83.3% and 86.7%, respectively, compared with those of non-prestressed slabs. However, it should be noted that the effectiveness of prestressing force grades (i.e. 50% and 70%) in cracks resistance is not much different. The presence of prestressing force also improved both load and energy dissipation of TRC slabs at the limit of deflection in serviceability.

The proposed FE models could accurately predict the load-carrying capacities and load-deflection relationships for the non-prestressed slabs. For the prestressed slabs, there were significant differences in cracking load between numerical models and test specimens. This could be explained by the reason that the prestressing force does not remain constant during the manufacturing process. The loss of stress in textile reinforcements was not well-controlled and also not implemented in ABAQUS models.

5. Declarations

5.1. Author Contributions

The basic theme of the research was discussed and decided by D.Q.N. and H.C.N. The manuscript was written by H.C.N. The results, discussions and conclusion section was completed by D.Q.N. and H.C.N. All authors have read and agreed to the published version of the manuscript.

5.2. Data Availability Statement

The data presented in this study are available in article.

5.3. Funding

The research is funded by the Ministry of Education and Training (Vietnam) under the grant number CT2020.04.GHA.05.

5.4. Acknowledgements

The authors would like to thank the University of Transport and Communications for support in the study.

5.5. Conflicts of Interest

The authors declare no conflict of interest.

6. References

[1] May, Sebastian, Oliver Steinbock, Harald Michler, and Manfred Curbach. “Precast Slab Structures Made of Carbon Reinforced Concrete.” Structures 18 (April 2019): 20–27. doi:10.1016/j.istruc.2018.11.005.

[2] Ngo, Dang Quang, Huy Cuong Nguyen, Dinh Loc Mai, and Van Hiep Vu. “Experimental and Numerical Evaluation of Concentrically Loaded RC Columns Strengthening by Textile Reinforced Concrete Jacketing.” Civil Engineering Journal 6, no. 8 (August 1, 2020): 1428–1442. doi:10.28991/cej-2020-03091558.

[3] Reinhardt, H. W., and M. Krüger. "Prestressed concrete plates with high strength fabrics." In PRO 39: proceedings of the sixth international RILEM symposium on fibre reinforced concretes (FRC)(BEFIB), RILEM Publications, Paris, (2004): 187-196.

[4] Krüger M., Reinhardt H., and Fichtlscherer, “Bond behaviour of textile reinforcement in reinforced and prestressed concrete,” Otto-Graf-Journal, (2001).

[5] Zdanowicz Katarzyna, Schmidt Boso, Naraniecki Hubert, Marx Steffen. “Bond behaviour of chemically prestressed textile reinforced concrete.” Conference: IABSE Symposium 2019 Guimarães "Towards a Resilient Built Environment", At: Guimarães, Portugal, (2019).

[6] Peled, Alva. “Pre-Tensioning of Fabrics in Cement-Based Composites.” Cement and Concrete Research 37, no. 5 (May 2007): 805–813. doi:10.1016/j.cemconres.2007.02.010.

[7] Du, Yunxing, Mengmeng Zhang, Fen Zhou, and Deju Zhu. “Experimental Study on Basalt Textile Reinforced Concrete under Uniaxial Tensile Loading.” Construction and Building Materials 138 (May 2017): 88–100. doi:10.1016/j.conbuildmat.2017.01.083.

[8] Gopinath, Smitha, Ravindra Gettu, and Nagesh R. Iyer. “Influence of Prestressing the Textile on the Tensile Behaviour of Textile Reinforced Concrete.” Materials and Structures 51, no. 3 (May 8, 2018). doi:10.1617/s11527-018-1194-z.

[9] Du, Yunxing, Xinying Zhang, Fen Zhou, Deju Zhu, Mengmeng Zhang, and Wei Pan. “Flexural Behavior of Basalt Textile-Reinforced Concrete.” Construction and Building Materials 183 (September 2018): 7–21. doi:10.1016/j.conbuildmat.2018.06.165.

[10] Du, Yunxing, Xinying Zhang, Lingling Liu, Fen Zhou, Deju Zhu, and Wei Pan. “Flexural Behaviour of Carbon Textile-Reinforced Concrete with Prestress and Steel Fibres.” Polymers 10, no. 1 (January 20, 2018): 98. doi:10.3390/polym10010098.

[11] Reinhardt, Hans W., Markus Krüger, and Christian U. Große. “Concrete Prestressed with Textile Fabric.” Journal of Advanced Concrete Technology 1, no. 3 (2003): 231–239. doi:10.3151/jact.1.231.

[12] H. W. Reinhardt, M. Krüger, Prestressed Concrete Slabs with High Strength Fabric, 6th RILEM Symposium on Fibre-Reinforced Concretes (FRC), (2004).

[13] Meyer C., Vilkner G., Glass concrete thin sheets prestressed with aramid fiber, PRO 30: 4th International RILEM Workshop on High Performance Fiber Reinforced Cement Composites (HPFRCC 4) RILEM Publications; Paris, France. (2003).

[14] Liu, Sai, Deju Zhu, Gaosheng Li, Yiming Yao, Yunfu Ou, Caijun Shi, and Yunxing Du. "Flexural Response of Basalt Textile Reinforced Concrete with Pre-Tension and Short Fibers Under Low-Velocity Impact Loads." Construction and Building Materials 169 (April 2018): 859–876. doi:10.1016/j.conbuildmat.2018.02.168.

[15] Du, Y.X., X. Shao, S.H. Chu, F. Zhou, and R.K.L. Su. "Strengthening of Preloaded RC Beams Using Prestressed Carbon Textile Reinforced Mortar Plates." Structures 30 (April 2021): 735–744. doi:10.1016/j.istruc.2021.01.024.

[16] Abbas, Eman, and Alaa H. Al-Zuhairi. "Non-Smooth Behavior of Reinforced Concrete Beam Using Extended Finite Element Method." Civil Engineering Journal 5, no. 10 (October 21, 2019): 2247–2259. doi:10.28991/cej-2019-03091408.

[17] Zulassung Z-31.10-182, Gegenstand: Verfahren zur Verstärkung von Stahlbeton mit TUDALIT (Textilbewehrter Beton), Prüfstelle: DIBt, Antragsteller: TUDAG TU Dresden Aktiengesellschaft, (2015).

[18] RILEM Technical Committee 232-TDT (Wolfgang Brameshuber). "Recommendation of RILEM TC 232-TDT: Test Methods and Design of Textile Reinforced Concrete." Materials and Structures 49, no. 12 (May 4, 2016): 4923–4927. doi:10.1617/s11527-016-0839-z.

[19] De Felice, Gianmarco, Maria Antonietta Aiello, Carmelo Caggegi, Francesca Ceroni, Stefano De Santis, Enrico Garbin, Natalino Gattesco, et al. "Recommendation of RILEM Technical Committee 250-CSM: Test Method for Textile Reinforced Mortar to Substrate Bond Characterization." Materials and Structures 51, no. 4 (July 9, 2018). doi:10.1617/s11527-018-1216-x.

[20] ABAQUS Manual, Analysis User's Manual 6.12, Dassault Systèmes Simulia Corp, Providence, Rhode Island, United States, (2012).

[21] EN 1992-1-1, Eurocode 2: Design of concrete structures - Part 1-1: General rules and rules for buildings, (2004).